

Dynamic Simulation of Adiabatic Catalytic Fixed-Bed Tubular Reactors: A Simple Approximate Modeling Approach

Wiwut Tanthapanichakoon ^{*,1}

Shinichi Koda ²

Burin Khemthong ³

¹ Dept. of Chemical Engineering, Graduate School of Science and Engineering, Tokyo Institute of Technology, Tokyo, Japan

² Ex-director, Sumitomo Chemical Engineering Co., Ltd. Nakase 1-chome, Mihama-ku, Chiba, Japan

³ Research and Development Center, SCG Chemicals, Bangkok, Thailand

*e-mail : wiwutt@chemeng.titech.ac.jp

Fixed-bed tubular reactors are used widely in chemical process industries, for example, selective hydrogenation of acetylene to ethylene in a naphtha cracking plant. A dynamic model is required when the effect of large fluctuations with time in influent stream (temperature, pressure, flow rate, and/or composition) on the reactor performance is to be investigated or automatically controlled. To predict approximate dynamic behavior of adiabatic selective acetylene hydrogenation reactors, we proposed a simple 1-dimensional model based on residence time distribution (RTD) effect to represent the cases of plug flow without/with axial dispersion. By modeling the nonideal flow regimes as a number of CSTRs (completely stirred tank reactors) in series to give not only equivalent RTD effect but also theoretically the same dynamic behavior in the case of isothermal first-order reactions, the obtained simple dynamic model consists of a set of nonlinear ODEs (ordinary differential equations), which can simultaneously be integrated using Excel VBA (Visual BASIC Applications) and 4th-order Runge-Kutta algorithm. The effects of reactor inlet temperature, axial dispersion, and flow rate deviation on the dynamic behavior of the system were investigated. In addition, comparison of the simulated effects of flow rate deviation was made between two industrial-size reactors.

Keywords: Dynamic simulation, 1-D model, Adiabatic reactor, Acetylene hydrogenation, Fixed-bed reactor, Axial dispersion effect

INTRODUCTION

The cracking of naphtha feedstock produces a stream composed of mainly

ethylene, some paraffins, diolefins, aromatics, and minute amount of acetylene. Ethylene is mainly used in the production of polymers, especially

polyethylene (PE). However, small amounts of acetylene, on the order of parts per million, are harmful to the catalysts used in polymerization (Schbib *et al.* 1996). Therefore, acetylene in the ethylene stream must be selectively hydrogenated with a minimum loss of ethylene. In the petrochemical industry there are two different routes for this ethylene purification: tail-end and front-end hydrogenation (Schbib *et al.* 1994). The most effective method for removing acetylene, down to 2-3 ppm, is selective hydrogenation over palladium catalysts in a multi-bed adiabatic reactor. The objective of this work is to develop a high-speed dynamic adiabatic 1-D model with/without axial dispersion for an industrial reactor of a tail-end acetylene hydrogenation system.

It has been reported that, at the end of a reactor run (shutdown for decoking) which is the worst condition, the maximum pressure drop across the reactor's bed length is about 0.2 bar, which is less than 1% of its operating pressure (about 35 bar) (Gobbo *et al.* 2004). This behavior is consistent with our plant data. Therefore, any change in reactor pressure may be considered insignificant and momentum balance can be omitted from our model. Gobbo *et al.* (2004) also reported that, at the exit of the first reactor, the largest temperature difference between the central point ($r = 0$) and peripheral point ($r = R$) was just 4.9 K. Therefore, radial temperature gradient needs not be considered in our model. Our preliminary investigation and simulation results show that, when commercial 100~200 micrometer thick egg-shell type

Pd/alumina catalyst is used, the retarding effect of intraparticle diffusion inside the catalyst pellet (3-4 mm in diameter) on the reaction rate is negligible and the effectiveness factor can be taken as essentially unity. The developed model aims to satisfactorily predict the outlet values and provide reasonable axial profiles of temperature and concentrations of acetylene, hydrogen, ethylene, and ethane in the reactor as functions of time. The effect of plug-flow with/without axial dispersion, as reflected by the change in residence time distribution (RTD) is accounted for in the model by a specific number of CSTR compartments connected in series. The effects of reactor inlet temperature, axial dispersion, and flow rate deviation on the dynamic behavior of the system will be investigated. In addition, comparison of the simulated effects of flow rate deviation will be made between two reactors of industrial scale.

Dynamic Model of Tubular Fixed-Bed Reactor

The unsteady-state multi-component mass and energy balance equations for a tubular fixed-bed reactor with only axial dispersion are derived as:

$$\frac{\partial c_{\alpha}}{\partial t} + \frac{\partial}{\partial z}(c_{\alpha}v_z) = D_{eff,\alpha} \left[\left(\frac{\partial c}{\partial z} \right) \left(\frac{\partial x_{\alpha}}{\partial z} \right) + c \frac{\partial^2 x_{\alpha}}{\partial z^2} \right] + \frac{\rho_p(1-\varepsilon)}{\varepsilon} r_{\alpha} \quad (1)$$

$$c\tilde{c}_p \left[\frac{\partial T}{\partial t} + \frac{\partial}{\partial z}(Tv_z) \right] = -\frac{\rho_p(1-\varepsilon)}{\varepsilon} \sum_{k=1}^m (\Delta H_{Rk}r_k) \quad (2)$$

In the case of plug flow, the effective dispersion coefficient $D_{eff,\alpha}$ becomes zero and the first term on the right-hand side of (1) will disappear. In principle, the above

coupled partial differential equations may be integrated numerically together with the appropriate kinetic rate expressions, and applicable initial and boundary conditions to obtain the system's dynamic behavior. Though various powerful sophisticated commercial software packages are available, the required computational time on a typical notebook PC is generally substantial. In addition, oftentimes the numerical integration or solution might run into numerical instability issue or fail to converge correctly. As an alternative, we have proposed and developed an approximate numerical approach which is not only fast but also makes use of widely available Microsoft Excel.

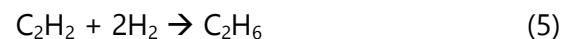
DERIVATION OF 1-DIMENSIONAL DYNAMIC MODEL

CSTR and plug-flow reactor (PFR) assume ideal flows with instantaneous complete mixing and piston movement, respectively. Generally, elements of fluid taking different routes through a reactor may require different lengths of time to pass through the vessel. The distribution of these times for the stream of fluid leaving the vessel is called the residence

time distribution (RTD) of the fluid. The RTD curve is needed to account for nonideal flow behavior, including axial dispersion effect in a plug-flow reactor (Levenspiel 1972). In theory, the RTD of a PFR can be obtained from the equivalent case of N tanks of CSTR connected in series, as N approaches infinity while the individual tank volumes approach zero and the total tank volume remains the same as that of the PFR. Similarly, the RTD of a PFR with axial dispersion of fluid can be approximated by a suitable finite number N of CSTRs in series. Here N is reasonably larger than 1. In practice, a series of 50 or more tanks usually gives an RTD sufficiently close to that of a PFR.

Selective Acetylene Hydrogenation Reactions (Mostoufi *et al.* 2005)

There are 3 major gas-phase reactions in this system (Bos *et al.* 1993, Westerterp *et al.* 2002):



Here we denote species $i = 1$ for C_2H_2 ; $i = 2$ for H_2 ; $i = 3$ for C_2H_4 ; and $i = 4$ for C_2H_6 . Since kinetic rate of reaction (5) is much slower than (3) and (4), it can be

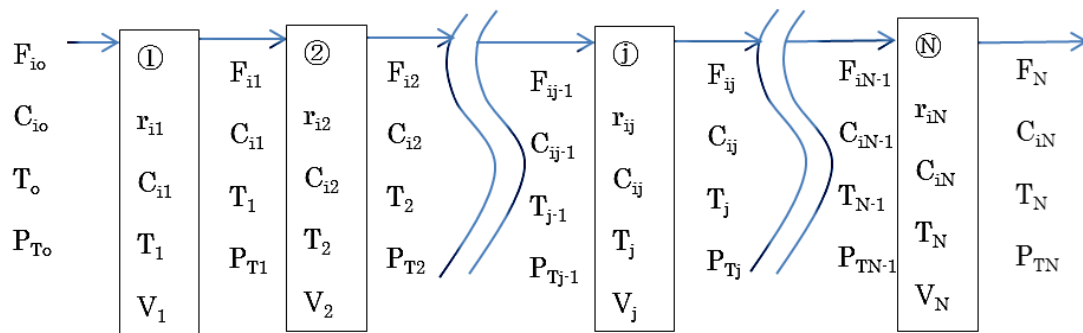


Fig. 1: Tubular fixed-bed catalytic reactor represented by a series of N CSTRs

disregarded here. The molecular weight of species i is: $M_1 = 26$ (acetylene), $M_2 = 2$ (hydrogen), $M_3 = 28$ (ethylene), $M_4 = 30$ (ethane).

Figure 1 illustrates the schematic diagram of a 1-D tubular fixed-bed reactor vessel *with axial dispersion*, as represented by a series of N CSTRs of equal volumes.

$$V_j = V_{\text{Tot}}/N = \Delta V = A\Delta z \quad (6)$$

The mass balance equation for species i ($i = 1, 2, 3, 4$) in compartment j ($j = 1, 2, \dots, N$) is given by

$$\begin{aligned} \frac{dC_{ij}}{dt} &= \frac{1}{\varepsilon\Delta V} (F_{ij-1} - F_{ij}) + \frac{\rho_c}{\varepsilon} r_{ij} \\ &= \frac{1}{\varepsilon\Delta V} (Q_{j-1}C_{ij-1} - Q_jC_{ij}) + \frac{\rho_c}{\varepsilon} r_{ij} \end{aligned} \quad (7)$$

The volumetric flow rate Q_j generally depends on the molar composition, pressure and temperature of the fluid stream. Strictly speaking, Q_j should be determined by solving the equation of motion. As a simplification, we assume here that there is no accumulation of total mass in any compartment j , even though there might be accumulation or depletion of moles of species i ($i = 1, 2, 3, 4$) in it. Therefore, for $j = 1, 2, \dots, N$:

$$Q_{j-1}C_{Tj-1}M_{avg\ j-1} = Q_jC_{Tj}M_{avg\ j} \quad (8)$$

Here $M_{avg\ j}$ is the average molecular weight of the fluid mixture in compartment j .

$$F_{Tj} = \sum_{i=1}^4 F_{ij} = Q_jC_{Tj} \quad (9)$$

$$C_{Tj} = \sum_{i=1}^4 C_{ij} \quad (10)$$

The reaction rate r_i is based on the kinetics obtained experimentally by Mostoufi *et al.* (2005) using a commercial catalyst Pd/Al₂O₃ (G58-B made by Sud-Chemie), as follows:

Rate of hydrogenation of acetylene C₂H₂ ($i = 1$ via (3)) [kmol/kg-cat·s] is

$$-r_1 = \frac{k_1 P_1 P_2}{[1 + K_1 P_3][1 + K_2 P_2]} \quad (11)$$

$$k_1 = 48.01 \exp(-146.8/T) \quad (12)$$

$$K_1 = 584.59 \exp(668.6/T) \quad (13)$$

$$K_2 = 2.855 \exp(404.3/T) \quad (14)$$

Rate of ethane production ($i = 4$ via (4)) by hydrogenation of ethylene C₂H₄ is

$$r_4 = \frac{k_2 P_3 P_2}{[1 + K_3 P_3]^{1.25} [1 + K_2' P_2]} \quad (15)$$

$$k_2 = 202.67 \exp(-4784/T) \quad (16)$$

$$K_3 = 0.0742 \exp(1502.7/T) \quad (17)$$

$$K_2' = 2.89 \exp(400/T) \quad (18)$$

Rate of generation of hydrogen ($i = 2$) is

$$r_2 = -r_4 + r_1 \quad (19)$$

Rate of generation of ethylene ($i = 3$) is

$$r_3 = -r_1 - r_4 \quad (20)$$

A second subscript j is added to eqns. (11) – (20) to specifically denote the condition in compartment j . Total pressure in compartment j (P_{Tj}) is given by

$$\begin{aligned}
 P_{Tj} &= \sum_{i=1}^4 P_{ij} = \sum_{i=1}^4 C_{ij} P_j / C_{Tj} \\
 &= \sum x_{ij} P_j
 \end{aligned} \quad (21)$$

From ideal gas law,

$$P_{ij} = \frac{n_{ij}}{\Delta V} R_g T_j = C_{ij} R_g T_j \quad (22)$$

The corresponding inlet and initial conditions are as follows:

Inlet of plug-flow reactor: $F_{T0} = Q_0 c_{T0}$ is given (23)

At $t = 0$, c_{ij} are given ($i = 1, 2, 3, 4; j = 1, 2, \dots, N$) (24)

$F_{i0} = Q_0 c_{i0}$ are given ($i = 1, 2, 3, 4$) (25)

Similarly, the thermal energy balance equation for the adiabatic reactor can be derived and summarized as follows. Note that axial and radial heat conduction may be ignored in this case.

$$\begin{aligned}
 &\frac{dT_j}{dt} \\
 &= \frac{1}{\varepsilon H_j} \left\{ \frac{1}{\Delta V} \left[H_{j-1} F_{Tj-1} T_{j-1} / C_{Tj-1} \right. \right. \\
 &\quad \left. \left. - H_j F_{Tj} T_j / C_{Tj} \right] \right. \\
 &\quad \left. + \rho_c [\Delta H_{R1} r_{1j} - \Delta H_{R2} r_{4j}] \right\} \\
 &\quad - \frac{T_j}{H_j} \frac{dH_j}{dt}
 \end{aligned} \quad (26)$$

$$\begin{aligned}
 &= \frac{1}{\varepsilon H_j} \left\{ \frac{1}{\Delta V} [H_{j-1} Q_{j-1} T_{j-1} - H_j Q_j T_j] + \right. \\
 &\quad \left. \rho_c [\Delta H_{R1} r_{1j} - \Delta H_{R2} r_{4j}] \right\} - \frac{T_j}{H_j} \frac{dH_j}{dt}
 \end{aligned}$$

For convenience sake, H_j and its time derivative are defined as

$$H_j = \sum_{i=1}^4 C_{ij} c_{pi} + \rho_c c_{p cat} \quad (27)$$

$$\frac{dH_j}{dt} = \sum_{i=1}^4 c_{pi} \frac{dC_{ij}}{dt} \quad (28)$$

The reactor inlet and initial conditions are given by

Inlet of reactor: T_o , P_{To} , C_{io} , Q_o or F_{To} ($i = 1, 2, 3, 4$) (29)

At $t = 0$, T_j , H_j are given ($j = 1, 2, \dots, N$) (30)

SIMULATION METHOD & CONDITIONS

Together with the relevant algebraic equations, the above set of non-linear first-order ODEs [equations (7), (26) and (28)] can be integrated numerically using 4th-order Runge-Kutta algorithm and Excel VBA (Visual BASIC in Applications). As a first step, only the first bed of a multi-bed reactor will be investigated. **Table 1** shows the input and parametric values used in the present investigation.

Note that the average MW of the feedstock is 27.9 kg/kmol, and the feed rate (base case) is 30.56 kg/s (1.0962 kmol/s; 0.78210 m³/s).

Property of catalyst: G58C, Pd-Ag/Al₂O₃
 Pellet size: 4.0 mm and 3.0 mm (equivalent diameter) for OPX and OPY, respectively
 Coating depth (shell thickness) of active

phase: 0.2 mm.

Catalyst pellet density: 1400 kg/m³;

specific surface area: ~30 m²/g

True density of Al₂O₃ (support): 3690 kg/m³

Pellet porosity = 62%

SIMULATION RESULTS AND DISCUSSION

Three independent simulation cases are investigated and discussed here.

Figure 2 shows the transient axial temperature profiles along the normalized reactor length for the *base case*. Before

steady state (SS) is reached, there is an overshoot of the reactor outlet temperature at time $t = 5s$. **Figure 3** shows the effect of inlet temperature T_{in} on the temperature profiles at $t = 1s$ and $10s$. Though omitted here, the magnitude of the overshoot is found to increase as T_{in} increases. In fact, if T_{in} is too high, the overshoot peak may increase exponentially to cause reaction runaway.

Figures 4 and **5** show the effect of T_{in} on the axial concentration profiles of C₂H₂ and C₂H₄, respectively. As expected, conversion of C₂H₂ is faster when T_{in} is

Table 1. Employed values of inputs and parameters

Variables/Parameters	Unit	Value
Acetylene (C ₂ H ₂)	%	1.5
Ethylene (C ₂ H ₄)	%	83.6
Ethane (C ₂ H ₆)	%	13.3
Hydrogen (H ₂)	%	1.6
Influent stream	kmol/s	1.0962 (base)
Reactor length (OPX: base)	m	OPX 2.73; OPY 3.35
Reactor diameter (OPX: base)	m	OPX 2.8; OPY 3.35
Inlet temperature	K	298 (base) 303,308,313
Inlet pressure	barA	21
Packing density of catalyst	kg/m ³	720
Bed voidage (ϵ)	m ³ /m ³	0.49
Compartment number (N)	—	50 (base), 20, 10

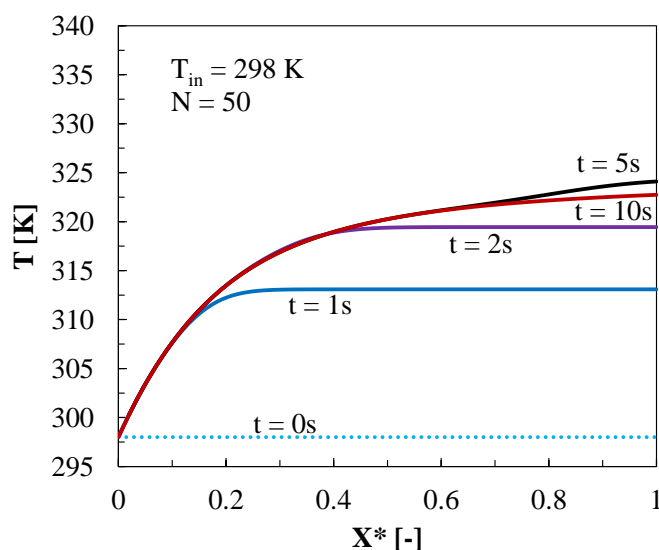


Fig. 2: Temperature profile (base case)

higher, and this difference is more pronounced at $t = 1\text{ s}$. Since the gas mixture volume expands when T_{in} is higher, the inlet concentration of C_2H_4 becomes lower, though the inlet composition and total flow rate remain constant. Nevertheless, its concentration profile at $t = 1\text{ s}$ is somewhat closer to the steady state when T_{in} is higher.

Simulation Case 2: Effect of number of tank compartments (N) (axial dispersion effect)

Figures 6 and 7 show the effect of axial dispersion on the temperature and C_2H_2 concentration profiles, respectively. The dispersion level increases monotonically as the total number of compartments N decreases from 50 (essentially plug flow)

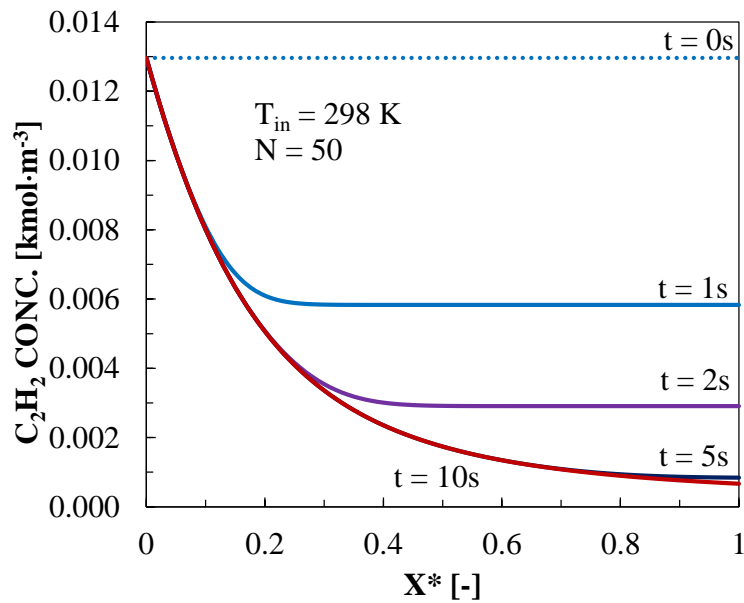


Fig. 3: C_2H_2 concentration profile (base case)

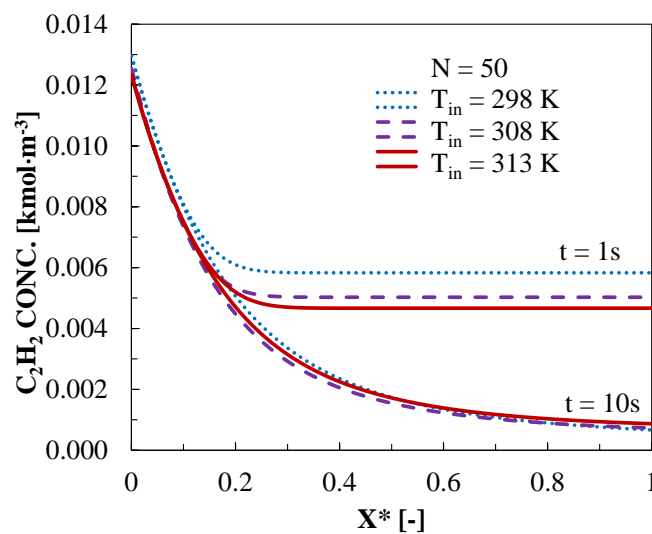


Fig. 4: Effect of T_{in} on C_2H_2 conc. profile

to 20 and 10. As expected, the profiles develop faster when the dispersion level increases, and this effect still slightly

remains after SS is reached. The conversion of C_2H_2 at reactor outlet is slightly reduced by axial dispersion effect.

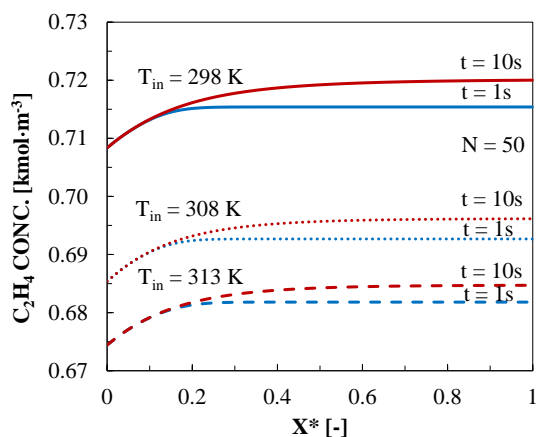


Fig. 5: Effect of T_{in} on C_2H_4 conc. profile

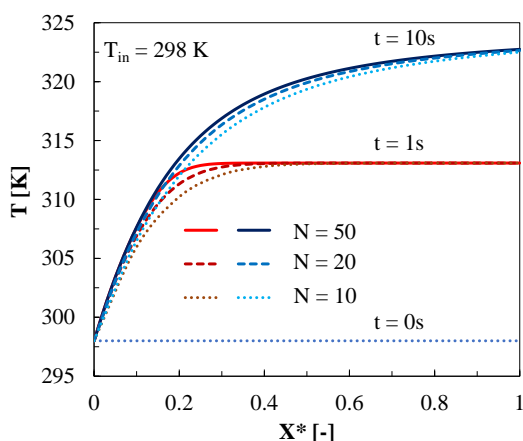


Fig. 6: Effect of N on temp. profile

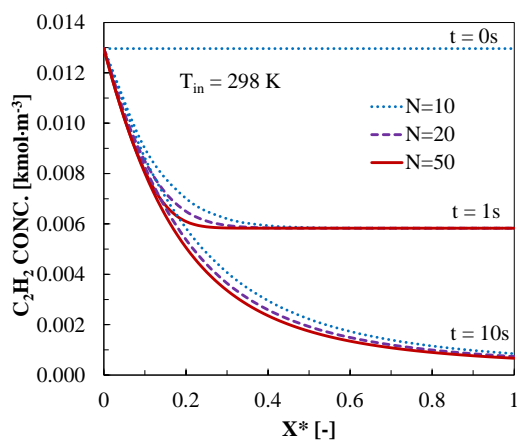


Fig. 7: Effect of N on C_2H_2 conc. profile

Simulation Case 3: Effect of influent flow rate on OPX and OPY reactors having different reactor configurations

Here -20% and +20% deviations in the total flow rate (flow ratio $F_R = 0.8$ and 1.2 , respectively) on the behavior of two commercial reactors of different sizes in olefins plants, code-named OPX and OPY, are investigated. As shown in **Table 1**, the reactors have different diameters and lengths, though they are operated under similar condition. **Figures 8 - 11** show that the SS temperature and C_2H_2

concentration profiles inside both reactors take somewhat a longer axial distance to become fully developed when total flow rate or F_R increases because of the resulting shorter residence time. As a result, **Figures 12** and **13** reveal that the total conversions of C_2H_2 and H_2 for the smaller OPX reactor become less than those of the larger OPY reactor, though OPX shows a higher selectivity of C_2H_2 conversion to C_2H_4 than OPY. Comparison between **Figures 8** and **9** reveals that the OPY reactor not only has a higher average

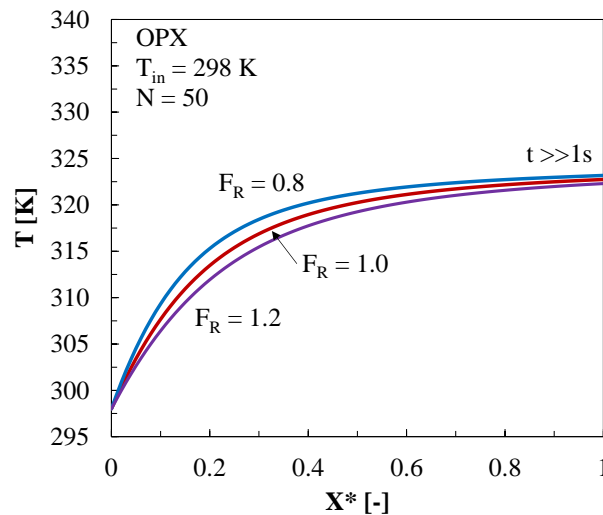


Fig. 8: Effect of F_R on OPX temp. profile

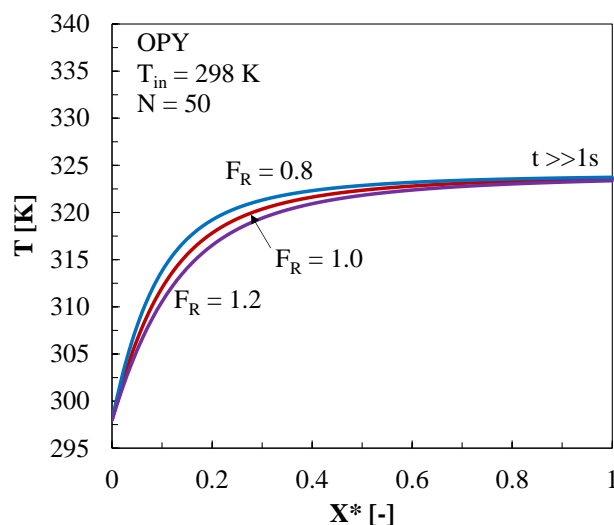


Fig. 9: Effect of FR on OPY temp. profile

temperature but its temperature also rises faster than OPX. This could be a root cause of the significantly faster catalyst deactivation rate observed in OPY.

CONCLUSIONS

Though fast and efficient to compute, the present model still has room for

improvement. The simulation results agree qualitatively with the plant data but not sufficiently quantitatively due to 2 reasons. First, the kinetic expressions given by Mostoufi *et al.* (2005) do not consider the presence of Ag promoter, or the role of CO in enhancing the acetylene hydrogenation selectivity, which existed in the said olefins

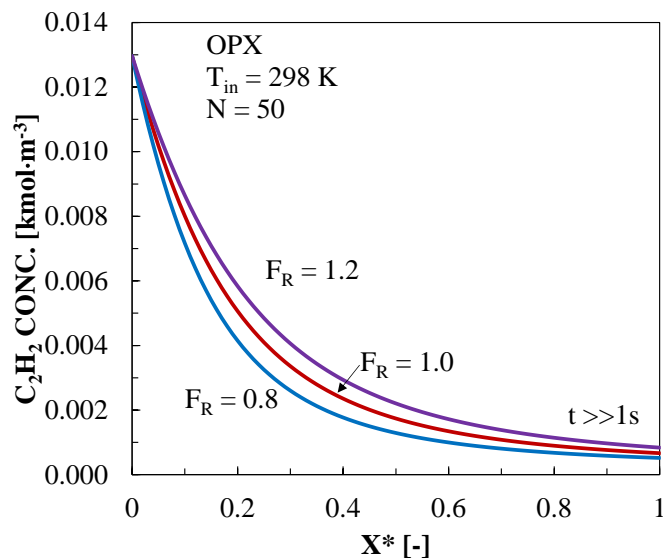


Fig. 10: Effect of F_R on OPX C_2H_2 conc. profile

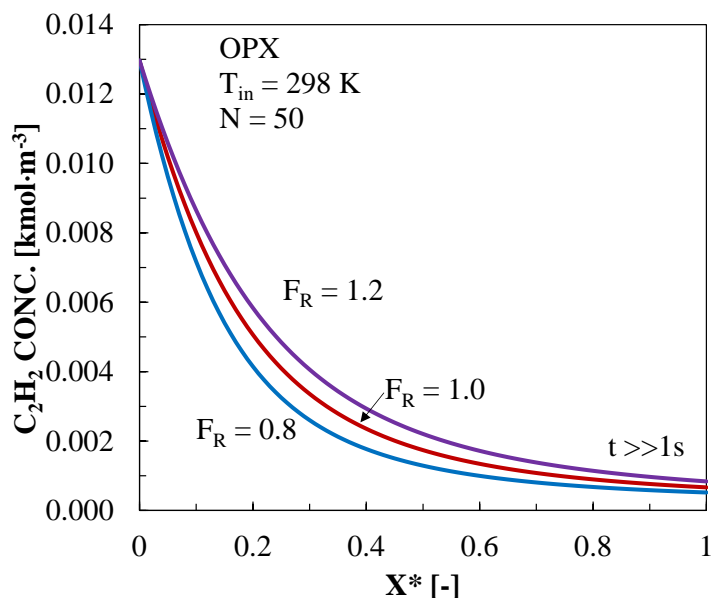


Fig. 11: Effect of F_R on OPY C_2H_2 conc. profile

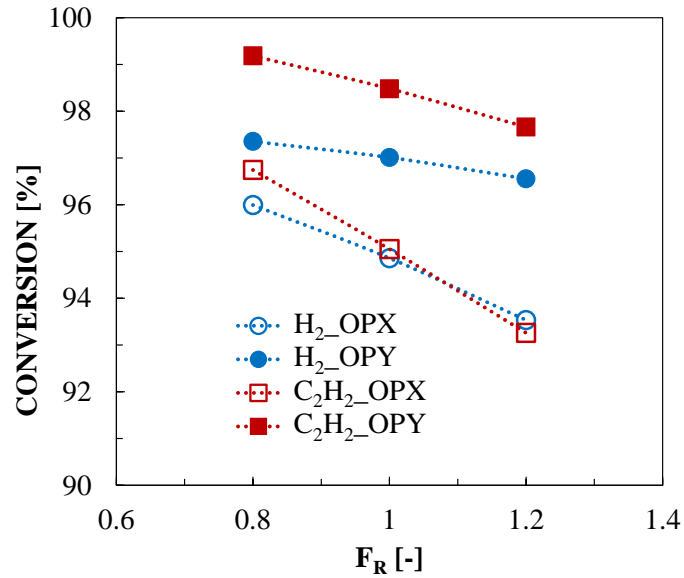


Fig. 12: Effect of F_R on OPX and OPY reactant conversion

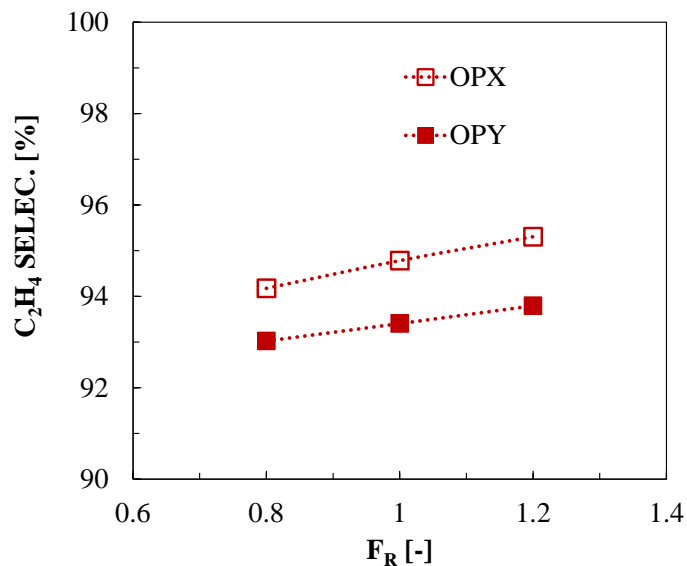


Fig. 13: Effect of F_R on OPX and OPY C₂H₄ selectivity

plants. Second, the use of RTD equivalent to a series of fully mixed compartments to take account of the axial dispersion in plug flow is theoretically proven to be exactly correct only in the case of isothermal first-order reaction system. Its application to a nonisothermal, nonlinear set of two parallel reactions can, therefore, be expected to give only approximate results. The authors will work to refine the kinetic

rate expressions for Pd-Ag/Al₂O₃ catalyst and improve our next predictions against plant data.

NOMENCLATURE

C_i : Concentration of species i
[kmol/m³-fluid]

C_{ij} : Concentration of species i in
reactor compartment j
[kmol/m³-fluid]

C_{Tj}	: Total molar concentration in compartment j [kmol/m ³ -fluid]	r_{ij}	: Rate of generation by reactions of species i in compartment j [kmol/kg-cat·s]
c_{pi}	: Specific heat of species i [kJ/kmol·K] (assumed independent of pressure)	r_i	: Rate of generation of species i [kmol/kg-cat·s]
c_{pcat}	: Specific heat of catalyst [kJ/kg-cat·K] (assumed to be constant)	T_j	: Temperature of fluid in reactor compartment j [K]
F_{ij}	: Molar flow rate of species i [kmol/s] out of compartment j (and into $j + 1$)	t	: Time [s]
F_{Tj}	: Total molar flow from compartment j [kmol/s]	V_j	: Volume of reactor compartment j [m ³] = $\frac{V_{Tot}}{N} = \Delta V$
H_j	: $\sum_{i=1}^4 C_{ij}c_{pi} + \rho_c c_{pcat}/\varepsilon$	x_{ij}	: Mole fraction of species i in compartment j [—]
ΔH_a	: Adsorption activation energy difference = $E_{adsorption} - E_{desorption}$ [kJ/mol]	z	: Axial distance along the reactor [m]
ΔH_{Rk}	: Heat of reaction of reaction no. k [kJ/kmol] ($k = 1$ for hydrogenation of acetylene; $k = 2$ for hydrogenation of ethylene) $\Delta H_{R1}^* @298\text{ K} = -172,000$ kJ/kmol; $\Delta H_{R2}^* @298\text{ K} = -137,000$ kJ/kmol	Δz	: Length of each tank compartment [m]
K_i	: Adsorption equilibrium constant for species i [bar ⁻¹]	Greek letter	
k_k	: Reaction rate constant of reaction k ($k = 1, 2$) [kmol/s·bar ²]	ε	: Bed voidage [—] or [m ³ -void/m ³ -bed]
P_i	: Partial pressure (absolute) of species i [bar]	ρ_c	: Packed density of catalyst [kg-cat/m ³ -bed]
P_{ij}	: Partial pressure (absolute) of species i in reactor compartment j [bar]	Subscripts	
P_{Tj}	: Total pressure in compartment j [bar]	o	: Inlet of reactor ($C_{ij0}, C_{io}, C_{To}, F_{io}, P_{To}, Q_o, T_o, T_{j0}$)
Q_j	: Volumetric flow rate from compartment j [m ³ /s]	REFERENCES	
R_g	: Gas constant = 8.314 [kJ/kmol·K] = 0.08314 [m ³ ·bar/kmol·K]	1. Bos, A.N.R. <i>et al.</i> (1993). "A kinetic study of the hydrogenation of ethyne and ethene on a commercial Pd/Al ₂ O ₃ catalyst", <i>Chem. Eng. Process: Process Intensif.</i> 32, 53–63.	
		2. Gobbo, R. <i>et al.</i> (2004). "Modeling, simulation, and optimization of a front-end system for acetylene hydrogenation reactors", <i>Braz. J. Chem. Eng.</i> 21, 545–556.	
		3. Levenspiel, O. (1972). <i>Chemical</i>	

Reaction Engineering, John Wiley & Sons.

4. Mostoufi, N. *et al.* (2005). "Simulation of an acetylene hydrogenation reactor", *Int. J. Chem. Reactor Eng.* 3, article A14.
 5. Schbib, N.S. *et al.* (1994). "Dynamics and control of an industrial front-end acetylene converter", *Comput. Chem. Eng.* 18, S355–S359.
 6. Schbib, N.S. *et al.* (1996). "Kinetics of Front-End Acetylene Hydrogenation in Ethylene Production", *Ind. Eng. Chem. Res.* 35, 1496-1505.
 7. Westerterp, K. R. *et al.* (2002). "Selective hydrogenation of acetylene in an ethylene stream in an adiabatic reactor", *Chem. Eng. Tech* 25, 529-539.
-